COBEM 2021 26th International Congress of Mechanical Engineering
November 22-26, 2021, Virtual Congress, Brazil

MODELING AND ANALYSIS OF BUBBLE PUMP PARAMETERS FOR A SOLAR-POWERED REFRIGERATOR BY DIFFUSION AND ABSORPTION FOR VACCINE STORAGE IN REGIONS WITHOUT ELECTRIFICATION

Rafael Teixeira Mendes
Luiz Machado
Márcio Fonte Boa Cortez
Pedro Antônio Diniz Chaves
Kássio Nogueira Cançado
Graduate Program in Mechanical Engineering - Universidade Federal de Minas Gerais, Av. Antônio Carlos, 6627, Belo Horizonte, MG, CEP: 31.270-901
rafaeltmendes@ufmg.br
luizm@ufmg.br
fonteboa@ufmg.br
pedrodinizch@gmail.com
kancado@ufmg.br

Fabiano Drumond Chaves
Department of Computing and Mechanics - Centro Federal de Educação Tecnológica, Rua José Peres, 558, Leopoldina, MG, CEP: 36.700-000
fabianodc@gmail.com

Abstract. *A small diffusion absorption refrigerator commonly used in hotel's rooms favors the conversion of its heat source to solar energy because the original heat source of the bubble pump is a 80 W electric resistor. The conversion of this power to the solar type can be done by replacing the electric resistor by a heat exchanger involving the bubble pump, inside which flows thermal oil heated in a concentrating solar collector. The two main objectives of the current work are the design of this heat exchanger and the analysis of thermohydraulic parameters of the system. This analysis was performed using a steady state model based on the application of energy and mass balance equations for thermal oil circulating into the heat exchanger of the bubble pump of a Dometic mini fridge loaded with ammonia, water and hydrogen. Equations were also applied to estimate the loss pressure along the oil circuit. The model, written in software EES (Engineering Equation Solver), was fed with the correlation of Churchil and Chu to evaluate the heat transfer between the oil and the external tube of the bubble pump, as well as with a temperature of 165ºC on the external wall of the bubble pump, whose value was obtained from experimental tests carried out in the refrigerator. The coaxial type heat exchanger has been designed with a length of 10 cm equal to that of the electric resistor of the refrigerator, and a diameter of 20 mm, which is 4 mm larger than the diameter of the outer tube of the bubble pump. Several thermal oils from the EES database were tested, of which the Therminol-VP1 was chosen as the most suitable for the heat exchanger operation. Therminol-VP1 allowed heat to be transferred at the rate of 80 W to the poor ammonia/water solution in the bubble pump with a mass flow rate of only 7,8 g.s^{-1}, resulting in a small pressure loss and an average temperature around 207°C in the oil circuit, a relatively low value that can be obtained in the concentrating solar collector.*

Keywords: *Diffusion absorption refrigerator, Bubble pump, Solar energy, Vaccine storage, Model, Heat transfer.*

1. INTRODUCTION

In recent years, several countries have applied policies to implement renewable energy sources in order to reduce the consumption of conventional fossil fuels that produce a significant amount of greenhouse gases. The generation of these renewable energies wind, solar, hydroelectricity, biomass and geothermal-based electricity has almost doubled worldwide between 1990 and 2010 (Carley *et al*., 2017). Specifically in Brazil, all regions have high levels of annual solar irradiation and great potential for solar energy generation, with the Northeast region of the country having the highest rates recorded (Pereira *et al*., 2017). Despite this, the use of solar energy in the country was the third lowest among renewable sources in 2020 (EPE, 2021).

Solar energy can be extremely useful in remote areas where populations do not have access to conventional electricity. In these regions, immunization programs become complex to be carried out with the same efficiency and safety as in urban regions, because immune biological generally need constant conservation at temperatures between 2°C and 8°C (Brazil, 2013).In this context, the use of diffusion absorption refrigerators (DAR) becomes an efficient solution because these machines operate with thermal energy that can be supplied by other renewable sources, including solar energy. In

addition, diffusion absorption refrigerators utilize natural refrigerants such as ammonia that have Global Warming Potential - GWP less than 1 (Calm and Hourahan, 2001).

Since when it was invented in 1928 by Von Platen and Munters, the diffusion absorption refrigeration cycle has been studied and improved by several researchers. Chaves *et al.* (2019) developed a mathematical model with experimental validation of an ammonia/water/hydrogen diffusion absorption refrigerator. Adjibade *et al.* (2017) developed a dynamic model for each component of the system and solved it numerically in order to predict transient state of the ammonia/water diffusion absorption refrigerator.

In addition to modeling studies of the original cycle, some adaptations of the DAR to operate with solar energy have also attracted researchers. Uppal *et al.* (1986) built a low-cost ammonia/water solar absorption refrigerator for vaccine storage. Abdulateef *et al.* (2008) made an optimum design for solar absorption refrigeration systems and compared the performances using ammonia/water, ammonia/lithium/nitrate and ammonia/sodium/thiocyanate solutions. Busso *et al.* (2011) analyzed theoretically and experimentally the integration of an ammonia/water diffusion absorption refrigerator with a solar concentrating collector.

For the above, the development of solutions that promotes the adaptation of diffusion and absorption refrigerators, dispensing the use of electricity, may represent an area of great interest. In this work, a thermohydraulic model is proposed for an annular heat exchanger with thermal oil in place of the electric resistor originally used in a commercial *Dometic* DAR with ammonia/water at pressure of 35 bars. Seven different types of thermal oils were tested, considering the operating power of 80 W of the cycle and a temperature of 160°C for the bubble pump wall. The length and diameter of the heat exchanger were defined and several thermohydraulic parameters necessary to guarantee the equipment operation regarding the energy demand of the refrigerator at maximum power were analyzed.

2. METHODOLOGY

The methodology used in the study was divided in two parts: (i) experimental tests to obtain the temperature on the bubble pump wall; (ii) mathematical model of the heat exchanger replacing the electric resistor of the bubble pump.

2.1 Experiment apparatus

Figure 1a shows the ammonia/water DAR scheme studied by Chaves *et al* (2019). The numbers of 1 to 9 on the figure represent the fluids states at the inlets and outlets of the refrigerator components, which were used by the authors to describe the corresponding refrigeration cycle. Heat is transferred in the generator of vapor (bubble pump) from an electric resistor, which promotes the production of ammonia and water vapors inside the refrigerator, generating upward movement of bubbles towards the rectifier. In this component, only water condenses, whose partial pressure implies a condensing temperature lower than that of ammonia, so that the liquid water returns by gravity to the bottom of the refrigerator, while ammonia vapor flows to the condenser. Figure 1b shows a picture of the ammonia/water DAR used in the present study, as well the thermocouples installed along the generator. To install these thermocouples, the insulation this component was removed, and after it was replaced (Figure 1c). The thermocouple readings, properly calibrated, were recorded using a *Minipa* digital thermometer with a resolution of 0.1°C.

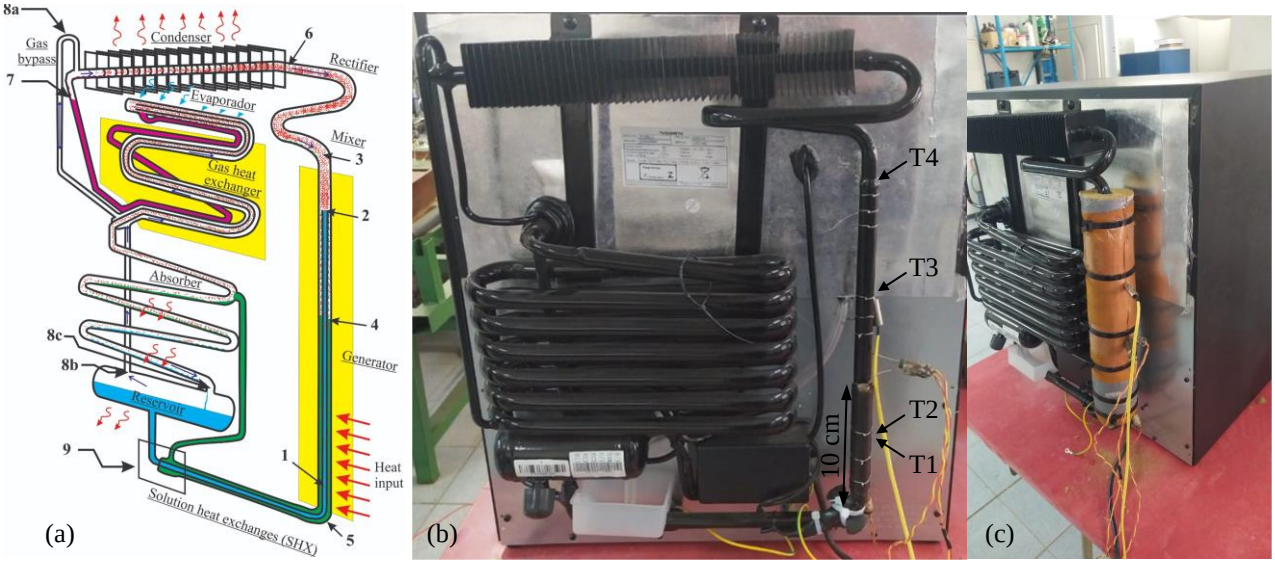

Figure 1: (a) Scheme of the ammonia/water DAR presented by Chaves *et al.* (2019). (b) Picture of the ammonia/water DAR instrumented and used in the present study. (c) Picture of the vapor generator with the insulation.

The temperature on the external wall of the generator is one of the input variables for the heat exchanger model. To estimate the evolution of this temperature during the operation of the refrigerator equipped with the electric resistor, four thermocouples were installed as shown in Figure 1b. Thermocouple T1 measures the temperature of the electric resistor 5 cm from its bottom, whose height is 10 cm. This thermocouple allowed evaluating when the resistor is turned on or off during the refrigerator operation. Thermocouples T2, T3 and T4, installed diametrically opposite the T1 thermocouple, measure the generator wall temperatures at positions 5 cm, 17.5 cm and 25 cm in relation to the bottom of the electric resistor. The indication of the T2 thermocouple is the most important because, after the stabilization of the refrigerator, it was used as input data for the heat exchanger model. Thermocouples T3 and T4 indicated temperatures much lower than those of the thermocouple T1 because the electric resistor does not directly supply heat to the generator above the 10 cm position. In addition, a fifth thermocouple was used to monitor the air temperature into the refrigerator.

2.2 Mathematical model

The purpose of this work was to evaluate the feasibility of replacing the electric resistor of an ammonia/water DAR by a tubular heat exchanger that uses thermal oil as secondary fluid. This evaluation was conducted with the support of a mathematical model of the heat exchanger. In view of the high viscosity of the oil and the low heat transfer rate in the vapor generator/bubble pump, and as consequence the low oil mass flow rate in the heat exchanger, the Reynolds number associated to the fluid flow is of the order of only 10^2, so that the flow is laminar. Furthermore, as the oil cross-sectional area in the annular space must be must be relatively large to avoid oil blockage, the effect of the forced convection on heat transfer process is negligible. Given the above, the heat exchanger model was developed considering the heat transfer between the oil and the vapor generator wall occurs exclusively by free convection.

2.2.1 Input and output variables

To replace electric resistor of the vapor generator, a tubular heat exchanger was designed. The Figure 2a shows the scheme of the heat exchanger proposed, whose secondary fluid is a thermal oil remotely heated in a solar collector. To guarantee the energy requirement of the system, the oil flow rate and temperature must be adjusted with aid of the heat exchanger model. The input and output variables of this model are shown in Figure 2b, including some geometric data. The heat exchanger has a length L = 10 cm, exactly equal to that of the electric resistor, and a diameter D_g = 15 mm corresponding to the generator tube. The diameter of the envelope tube D_e was set at 20 mm to ensure a larger cross section area in order to avoid blockage of the oil flow. In addition, a greater value for this diameter will imply a small loss pressure of the oil flowing through the system. Other input variables are the heat transfer rate q from the oil to the generator wall, the temperature T_g of this wall and the temperature difference ΔT_o of the oil between the inlet the outlet of the heat exchanger. From refrigerator manufacturer, q = 80 W, while T_g was found experimentally, as presented in the next section. A low ΔT_o = 5°C was set to ensure heat distribution more uniform along the heat exchanger, similar to that provided with the electric resistor. The output variables of the model are oil mass flow rate (m) and its inlet and outlet temperatures T_{o1} and T_{o2}, as well as the loss pressure ΔP_o in heat exchanger. The type of oil used is also an output variable of the model. Different oils were tested until finding one that at the lowest possible temperature can transfer heat at the rate of 80 W to the system. It is also important to verify if the selected oil will remain as liquid under the system operating conditions. Thus, another important output variable of the model is the oil saturation pressure (P_{vap}) at the highest oil temperature, which is the inlet temperature of the fluid in the heat exchanger (T_{o1}).

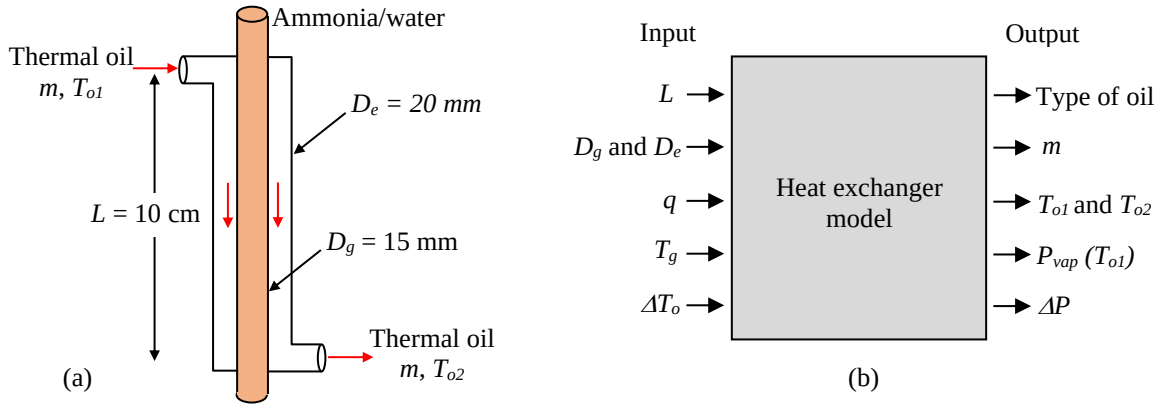

Figure 2: (a) Scheme of the heat exchanger. (b) Input and output variables of the heat exchanger model.

2.2.2 Energy equations

The heat transfer rate q in the heat exchanger can be calculated from Eq. (1) and Eq. (2) presented below. In the first equation, m and C_p are the mass flow rate and specific heat of the oil and T_{o1} and T_{o2} are the inlet and outlet temperatures of this fluid in the heat exchanger. In the second equation, h is the heat transfer coefficient by free convection between the oil and the vapor generator wall. The first term in parentheses is the heat exchange surface, which is function of the diameter D_g and length L of the heat exchanger. T_o is the oil average temperature, defined by the arithmetic mean of the temperatures T_{o1} and T_{o2}, and T_g is the temperature of the generator wall at the middle height of the heat source region.

$$q = mc_p(T_{o1} - T_{o2}) \tag{1}$$

$$q = h\,(\pi\, D_g\, L)\big(T_o - T_g\big) \tag{2}$$

The coefficient h of free convection was estimated by the Churchill and Chu correlation [1975], given by Eq. (3). As the hydraulic diameter in the annular of the heat exchanger is relatively large, the generator tube can be treated as a vertical plate of height L, in which case this correlation can be applied. In the Eq. (3), K is the thermal conductivity and Pr is the Prandtl number of the oil, both calculated at the film temperature, defined by the arithmetic mean between T_o and T_g. Another term in this equation is the Rayleigh number, Ra, given by Eq. (4). The vertical length L of the heat exchanger is the characteristic dimension in Eq. (4) and Eq. (3). In the Eq. (4), the terms not yet mentioned are the local gravity acceleration (g) and the coefficient of thermal expansion (β), density (ρ) and dynamic viscosity (μ) of the oil, which values must be calculated at the film temperature.

$$\sqrt{\frac{h\,L}{K}} = 0.825 + \frac{0.387\,Ra^{1/6}}{\left[1 + \left(\frac{0.492}{Pr}\right)^{9/16}\right]^{8/27}} \tag{3}$$

$$Ra = \frac{g\,\beta\,\rho\,\big(T_g - T_o\big)L^3}{\mu} \tag{4}$$

2.2.3 Pressure loss equations

Pressure loss along the oil circuit of energy consuming also was estimated. The Figure 3 shows this circuit, which consists of the heat exchanger of the generator/bubble pump, oil reservoir, gear pump, and pipes of connection. Figure 3 shows also the circuit of energy generation, although it is not part of the scope of this work.

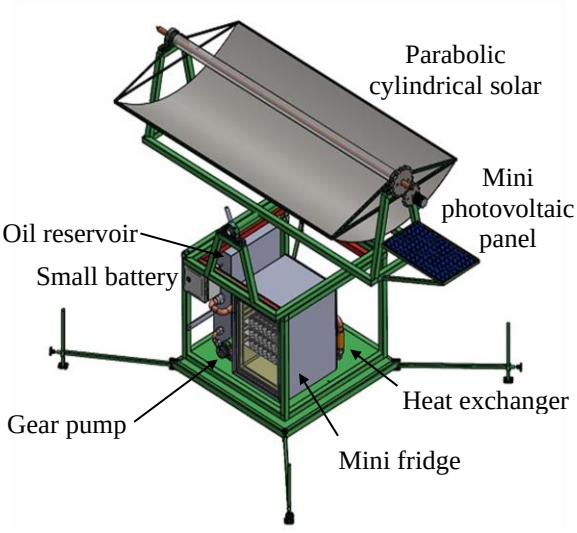

Circuit of energy consuming
- Oil reservoir: 35 liters
- Heat exchanger: L = 10 cm and $D_{hyd} = D_e - D_g$
  D_{hyd} is the hydraulic diameter of the annular space with diameters D_g = 15 mm and D_e = 20 mm
- Pipes: L = 3.0 m and D = 6 mm
- Gear pump: 0 to 1.0 liters/minute

Circuit of energy generation
- Reservoir volume
- Solar collector tube
- Pipes

Figure 3: Components of the oil circuits for generation and consuming of energy of the solar refrigerator.

The pressure loss along the pipes and heat exchanger was estimated by the Eq. (5), while the Eq. (6) was used to estimate the pressure loss at the entrances and exits of the oil reservoir and heat exchanger. In the Eq. (5), f is the friction factor for a laminar flow, given by the ratio between 64 and the oil Reynolds number. L and D are the lengths and diameters of the pipes and heat exchanger, presented in Figure 3, G is the oil mass flux, defined by the ratio between the

oil mass flow rate and the cross section area where the oil flows, and ρ is the oil density. In the Eq. (6), K_{ent} is a coefficient associated to the pressure loss in a sudden expansion (e.g. entrance of the oil reservoir) or sudden contraction (e.g. exit of the reservoir) and V is the oil average velocity in the pipe cross section upstream of the expansion or downstream of the contraction. Although the factor K_{ent} varies from 0 to 1, depending of the ratio of areas of the cross sections involved in these transitions, the value equal to 1 was adopted in order to make the analysis of the problem more conservative. Tables and graphs with specific values of K_{ent} can be found in Pritchard (2011).

$$\Delta P_{st} = f \frac{L}{D} \frac{G^2}{2\rho} \tag{5}$$

$$\Delta P_{ml} = K_{ent} \frac{V^2}{2} \tag{6}$$

Equation of the model were solved using the software EES (Engineering Equation Solver). In the next section, the results obtained from simulations carried out with the model are presented. In addition, experimental results obtained from DAR instrumented with thermocouples are also explored.

3. RESULTS

In this section, the following results on the parameters of the circuit of energy consuming are discussed: wall temperature of the vapor generator/bubble pump, diameter of the envelope tube of the heat exchanger, thermal oil mass flow rate, type of oil used, and the pressure loss associate to the flow along the oil circuit.

3.1 Generator wall temperature

Wall temperature of the generator in the heat source region is a very important parameter because it is an input variable of the heat exchanger model. From the experimental tests, this temperature remained around 160ºC during a stable refrigerator operation, as presented bellow. This value is consistent, considering data obtained from the manufacturer: operating pressure of 35 bars and masses of ammonia and water equal to 100 g and 180 g, respectively, representing a global concentration of ammonia equal to 36%. At this pressure, from the IIR Table (1994), the poor solution of ammonia/water at concentration of 30% presents an equilibrium temperature close of 160°C. Therefore, the generator external wall a little above of 160ºC can transfer heat to the solution inside the generator/bubble pump. Despite the small temperature difference between the wall and the solution, a heat transfer rate of 80 W is guaranteed by the high internal convective coefficient resulting from the boiling of ammonia and water.

Figure 4 shows the temperature evolutions obtained from five thermocouples installed in the refrigerator, as explained in Section 2. The thermocouples T1 and T2 provide the temperatures of the electric resistor and generator wall in the heat source region. The thermocouples T3 and T4 give the temperatures of the wall generator just above the electric resistor top. The fifth measurement is the air temperature inside the refrigerator. Figure 4a shows the temperatures evolutions during the first 30 minutes of refrigerator operation after the refrigerator was turned on, while Figure 4b shows these evolutions from 30 to 400 minutes.

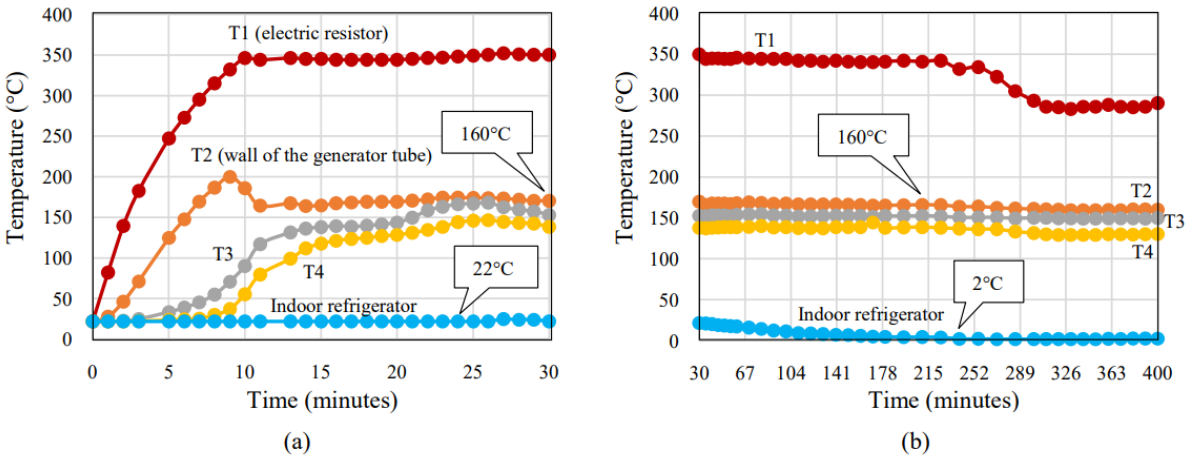

Figure 4: Temperature evolutions in the vapor generator during refrigerator operation.

After the start of the system, with the exception of the air temperature inside the refrigerator, the others changed rapidly, increasing during the first 30 minutes of refrigerator operation, when the lectures of the thermocouples T1, T2, T3 and T4 stabilized at approximately 350°C, 160°C, 150°C and 140°C, respectively. Only from that moment on, the air temperature inside the refrigerator started to change, decreasing of 22°C to 2ºC at the instant time 250 minutes. Until that moment, the other temperatures remained almost unchanged. Then, the electric resistor was automatically turned off by the action of the internal refrigerator thermostat, implying a drop in temperature indicated by thermocouple T1, followed by minor reductions in temperatures indicated by the thermocouples T2, T3 and T4, as well as by a small increase in temperature inside the refrigerator. Around 400 minutes, the electric resistor was automatically turned back on. After this moment, although not shown in Figure 4, the temperatures of the thermocouples installed on the generator wall indicated discrete variations either when the resistor was turned on or off.

3.2 Heat exchanger diameters

In this study, the tube diameter of the vapor generator (D_g) is 15 mm, but the diameter of the envelope tube (D_e) involving the generator in the heat source refining must be chosen. To assist in choosing, seven thermal oils from the EES database were tested, called for Therminol 55, 59, 66, 72, LT, VP1, and XP. Table 1 presents some physic properties of these oils at a temperature of 200ºC: density (ρ), dynamic viscosity (μ), heat specific (Cp), thermal conductivity (K), Prandtl number (Pr), thermal expansion coefficient (β), and pressure of vapor (P_{vap}). On the other hand, Figure 4 shows the variation of the oils Reynolds numbers as a function of the diameter envelope tube. The Reynolds number was calculated by Eq. (7), in which G is the oil mass flow, given by the ratio between the oil mass flow rate and the cross-sectional area in the annular space, D_{hyd} is hydraulic diameter of the annular space of the heat exchanger, given by the difference between D_g and D_e, and μ is the oil dynamic viscosity. All curves shown in Figure 5 were obtained for a oil mass flow rate calculated by Eq. (1), in which the heat transfer rate q is 80 W, value given by the refrigerator manufacturer, and the oil temperature difference through the heat exchanger ($T_{o1} - T_{o2}$) was fixed at 5ºC for all seven oils. The physic properties of the oils were taken at a temperature of 200ºC.

$$Re = \frac{G\, D_{hyd}}{\mu} \tag{7}$$

Table 1: Physic properties of thermal oils from the EES database.

Physics properties	Therminol						
	55	59	66	72	LT	VP1	XP
ρ [Kg/m³]	748	839	885	916	706	913	761
μ [10^{-5} N.s/m²]	74.7	47.6	85.9	49	19.1	39.5	83.9
Cp [kJ/(kg.°C)]	2.55	2.28	2.20	2.04	2.45	2.05	2.60
K [kW/(m.°C)]	107	104	106	118	88.6	114	113
Pr	17.7	10.4	17.9	8.47	5.28	7.10	19.3
β [10^{-4} °C^{-1}]	9.73	9.75	8.22	9.83	14.2	9.87	9.56
P_{vap} [kPa]	2.21	13.4	2.28	31.9	167	24.0	1.76

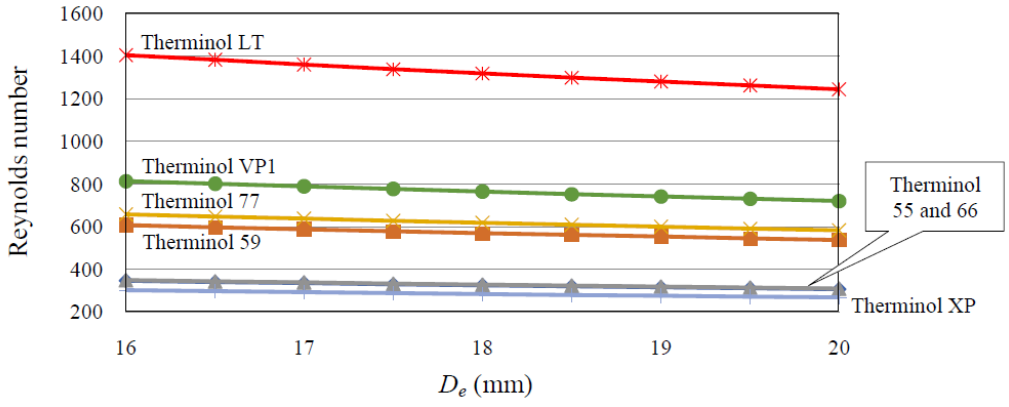

Figure 5: Reynolds number in function of the envelope diameter of the heat exchanger.

From the analysis of the Figure 5, it is observed that all oils present a low value of the Reynolds number, therefore not enough for that the effect of forced convection on the heat transfer of the oil to the vapor generator wall to be

significant. In addition, from Figure 5, it is also concluded that the effect of the envelope tube diameter on the Reynolds number is small. Only a value of this diameter very close to the diameter of 15 mm of the vapor generator could generate a high Reynolds number capable of implying significant forced convection. However, the cross section area of the heat exchanger would be very small, so there would be blockage in the oil flow. Therefore, the envelope tube diameter of the heat exchanger was set at 20 mm for the simulations performed with the model presented at the end of this section.

3.3 Thermal oil selection

The next step is the selection of the oil to be used as the secondary fluid for the heat exchanger. The best choice is the oil with the highest heat transfer coefficient, therefore the fluid that will provide the lowest temperature of operation of the energy consuming circuit. This is very important for the power generation circuit to also operate at lower temperature, under the risk of the oil very hot stored in the reservoir losing heat to the environment at a very high rate, implying a solar collector with an evacuated tube and a reservoir of oil with an insulation of great thickness. In these circumstances the cost of manufacturing the system would be very expensive.

From the analysis of the Figure 5, Therminol LT has the highest Reynolds number, around 1300. However, as previously discussed, this value is not sufficient to promote a significant effect of forced convection. In addition, this oil has high vapor pressure, above atmospheric pressure, so the fluid tends to form vapor at the gear pump suction, causing cavitation in this device. Thus, this oil could only be used at lower temperatures, therefore incompatible with the need of a minimum temperature of 160ºC for the vapor generator wall. On the other hand, other oils (Therminol 55, 59, 77, VP1, and XP) are selectable because their vapor pressures are low. From a more superficial analysis of Eq. (3) and Eq. (4), Therminol VP1 seems to provide the highest heat exchange coefficient. First, although the thermal expansion coefficient has an important influence on the heat transfer, the six selectable oils have similar value for this property. In fact, Therminol VP1 has the highest heat transfer coefficient mainly because it has the highest density and lowest dynamic viscosity, whose combination impacts positively the heat transfer. Although thermal conductivity has a minor influence on the heat exchange coefficient, another point favorable to the Therminol VP1 is that this oil is the best heat conductor of all. Finally, on the influence of the Prandt number, a higher value favors the heat exchange, so this aspect is unfavorable to the Therminol VP1. However, the Prandtl number influence is small on the heat exchange coefficient.

To confirm the oil Therminol VP1 as the most indicated to be used in the system, the heat exchanger model was run with the aid of the EES software considering the following input variables: q = 80 W, ΔT_o = 5°C, and T_g = 165°C. In addition, the following geometric data were used: L = 10 cm, D_g = 15 mm, and D_e = 20 mm. Table 2 shows the results obtained for all selectable oils, whose values in the four first columns are the mass flow rate of the oil (m), its input and output temperatures (T_{o1} and T_{o2}), and the heat transfer coefficient (h) between the oil and the generator wall. The pressure of vapor (P_{vap}) and the loss pressure (ΔP) of the oil along the system are presented in the two last columns. As expected, Therminol VP1 was the fluid that transferred heat to the vapor generator/bubble pump with the lowest oil temperature level because it presented the highest heat transfer coefficient of all, although Therminol 72 also has operated at a lower temperature. Both have the highest evaporating pressures, but these values are only third of the atmospheric pressure around which the oil is pumped. Therefore, there is no risk of cavitation occurring in the oil pump.

Table 2: Physic properties of thermal oils from the EES database.

Oil	m [g/s]	T_{o1} [°C]	T_{o2} [°C]	h [W/(m².°C)]	P_{vap} [kPa]	ΔP (kPa)
Therminol 55	6.15	219.0	214.0	329.5	3.38	3.90
Therminol 59	6.90	215.1	210.1	356.7	17.3	2.54
Therminol 66	7.09	220.8	215.8	318.4	3.55	4.32
Therminol 72	7.75	211.3	206.3	387.6	35.5	2.83
Therminol VP1	7.75	209.7	204.7	402.6	27.5	2.23
Therminol XP	6.00	220.2	215.2	322.2	2.84	4.16

3.4 Loss pressure

It remains to calculate the pressure drop that selectable oils generate in the system. This value is also added in Table 2, from which it is observed that all oils have a pressure loss between 2.2 kPa and 4.2 kPa. Thus, considering an oil pump discharge pressure of 90 kPa (atmospheric pressure at the local where the solar refrigerator is being studied), the pump suction pressure will be around 85 kPa, which is a value much higher than the vapor pressure of Therminol VP1 oil and others at the temperature de system operation. Therefore, there is no risk that any of the oil will cause cavitation in the pump. Still on this pump, and from first column of the Table 2, the oil mass flow rate imposed by this device is 7.75 g/s, implying a volumetric flow of 0.51 liter/minute. Considering that the oil flow must be variable within a small range in order to adjust the storage temperature of vaccines inside the refrigerator, the gear pump must be driven by a frequency inverter capable of modulating the volumetric flow from 0 to 1 liter/minute.

4. CONCLUSIONS

The main objective of this work was to design a heat exchanger using a thermal oil as a secondary fluid to replace the electric resistor as a heat source in a refrigerator by adsorption and absorption (DAR), charged with ammonia, water and hydrogen, in order to use the refrigerator for storage of vaccines in regions without electrification. The oil is heated by a parabolic cylindrical solar collector. The proposed heat exchanger is of the tubular type and mounted coaxially with the vapor generator of the refrigerator.

A thermohydraulic model was developed and written in Engineering Equation Solver (EES) to determine some system parameter, such as the type of oil, the temperature level and the pressure loss throughout the oil circuit, which is consisting of the heat exchanger, an oil pump, a storage oil reservoir, and pipes connecting these elements. An analysis of the heat transfer mechanisms revealed that free convection is predominant for the oil heating the vapor generator wall, and the Churchill and Chu correlation was used to calculate the heat transfer coefficient from the oil to this wall. Experimental tests were carried out on a mini fridge DAR to determine the temperature 160°C on the refrigerator generator wall, which is one of the input variables of the model.

From simulations carried out with the model, seven thermal oils from the EES database were stated. The fluid chosen to be the secondary fluid of the heat exchanger was the oil Therminal VP1, since this fluid had the highest heat transfer coefficient and, therefore, the lowest temperature level, implying a more efficient operation of the solar collector. From the analysis of the pressure loss in the system and considering the oil vapor pressure, it was concluded that there is no risk of the Therminol VP1 causing cavitation at the oil pump suction.

Finally, from the results obtained, it was concluded that the solar cooler assembly should be assembled with the following guidelines: (i) steam generator heat exchanger with a length of 10 cm and annular space diameters of 15 mm and 20 mm; (ii) flow rate imposed by the oil pump of 0 to 1.0 liter/minute; (iv) 35 L reservoir with oil at 220ºC; (v) Thermal oil Therminol VP1 or similar fluid.

5. ACKNOWLEDGEMENTS

This work was supported by National Council for Scientific and Technological Development (CNPq), Coordination of Improvement of Higher Level Personnel (CAPES), Foundation for Research Support of the State of Minas Gerais (FAPEMIG), and Research Development Foundation (FUNDEP).

6. REFERENCES

Abdulateef, J.M.; Sopian, K.; Alghoul, M.A., 2008 “Optimum design for solar absorption refrigeration systems and comparison of the performances using ammonia-water, ammonia-lithium nitrate and ammonia-sodium thiocyanate solutions.” *International Journal of Mechanical and Materials Engineering*, Vol. 3, No.1, 17-24.

Adjibade, M. I. S., Thiam, A., Awanto, C., Baye A.N., Sambou V., 2017 “Dynamic investigation of the diffusion absorption refrigeration system NH3-H2O-H2”. *Case Studies in Thermal Engineering.* Vol. 10, p. 468-474.

Brazil. Ministry of Health. Secretariat of Health Surveillance. Department of Epidemiological Surveillance. *Manual of Cold Chain* – 4. ed. – Brasília: Ministry of Health, 2013.

Busso, A., Franco, J., Sogari, N., &Cáceres, M., 2011 “Attempt of integration of a small commercial ammonia-water absorption refrigerator with a solar concentrator: Experience and results”. *International Journal of Refrigeration*, Vol. 34(8), p. 1760–1775.

Calm, J. M. and Hourahan, G. C., “Refrigerant Data Summary”. *Engineered Systems*, 18(11):74-88, November 2001.

Carley, S., Baldwin, E., MacLean, L.M., Brass, J.N., 2017. “Global expansion of renewable energy generation: An analysis of policy instruments”. *Environmental and Resource Economics*. Vol. 68, pp. 397–440.

Chaves, F.D.; Moreira, M.F.S.; Koury, R.N.; Machado, L.; Cortez, M.F.B. 2019 “Experimental study and modeling within validation of a diffusion absorption refrigerator”. *International Journal of Refrigeration*, v. 101, p. 136-147.

Churchill, S.W., and H.H.S. Chu, 1975. “Correlating Equations for Laminar and Turbulent Free Convection from a Vertical Plate.” *International Journal of Heat and Mass Transfer*, Vol. 18, pp. 1323-1329.

EPE, 2021, *Brazilian Energy Balance 2020*, *Summary Report* (in Portuguese), Empresa de Pesquisa Energética EPE, Rio de Janeiro, epe.gov.br/sites-pt/publicacoes-dados-abertos/publicacoes/PublicacoesArquivos/publicacao-601/topico-588/Relat%C3%B3rio%20S%C3%ADntese%20BEN%202021-ab%202020_v2.pdf. Accessed 12 January 2021.

$NH_3 – H_2O$ Thermodynamics and physical properties, 1994. International Institute of Refrigeration.

Pereira, E. B.; Martins, F. R.; Gonçalves, A. R.; Costa, R. S.; Lima, F. L.; Ruther, R.; Abreu, S. L.; Tiepolo, G. M.; Pereira, S. V.; Souza, J. G. *Atlas brasileiro de energia solar*. 2.ed. São José dos Campos: INPE, 2017. 80 p.

Pritchard, P. J.; Leylegian, J. C. *Introduction to Fluid Mechanics*. 8th ed. John Wiley & Sons, INC, Hoboken, New Jersey, USA, 2011.896 p.

Uppal, AH., Norton, B. and Probert, SD., 1986. “A low cost solar-energy stimulated absorption refrigerator for vaccine storage”. *Appl Energy*, Vol. 25, pp. 167-74.

Von Platen, B.C., Munters, C.G. US Patent 1, 685,764, 1928.

7. RESPONSIBILITY NOTICE

The authors are the only responsible for the printed material included in this paper.